11th World Congress on Computational Mechanics (WCCM XI)
5th European Conference on Computational Mechanics (ECCM V)
6th European Conference on Computational Fluid Dynamics (ECFD VI)
E. Oñate, J. Oliver and A. Huerta (Eds)

DESIGN AND ANALYSIS OF 3D WOVEN COMPOSITES AT FAILURE

DAVID EHRLICH, HARUN BAYRAKTAR, JON GOERING, MICHAEL MCCLAIN, AND CHRIS REDMAN

Albany Engineered Composites, 112 Airport Drive, Rochester, NH 03867, USA

e-mail: david.ehrlich@albint.com, www.albint.com/aec

Key Words: *3D woven, Composites, Strain Softening, Damage, Aerospace, Automotive.*

Abstract: 3D woven composites have superior fracture toughness, fatigue life, and damage tolerance compared to laminated composites due the presence of through-thickness reinforcement. These properties lead to high specific energy absorption, enabling the manufacturing of 3D woven composite parts that can replace traditional high strength metal ones, at a lighter weight. The goal of this study was to develop a macro-scale, i.e. continuum level, finite element material model to predict the progressive failure and energy absorption of 3D woven composites. Most material properties used in the model developed can be calibrated from standard experimental setups. Since the characterization of failure includes regions of softening behavior, a characteristic length scale is present in the model as to prevent the incidence of pathological mesh dependence. For validation, this material model was then used in a macro-scale finite element analysis to predict the maximum load and energy absorption of a 3D woven composite beam subjected to 3-point bending. The model predictions were in close agreement with experimental data for samples manufactured and tested as part of this study.

1 INTRODUCTION

3D woven composites have superior fracture toughness, fatigue life, and damage tolerance compared to laminated composites due the presence of through-thickness reinforcement (Figure 1) [1]-[4]. These properties lead to high specific energy absorption of 3D woven composites, enabling the manufacturing of parts suitable to replace the traditional high strength metal ones used in the aerospace and automotive industries, at a lighter weight. In addition, 3D weaving technology allows for the tailoring of the reinforcement architecture and fiber content to meet performance requirements and also produces a preform woven in a near-final shape, reducing complexity and cost of manufacturing [5].

Computer Aided Design (CAD) and Engineering (CAE) of composite parts using numerical structural analysis tools such as Finite Element Analysis (FEA) is increasingly common due to its reduced cost and development iteration cycle time. However, all such commercially available tools are limited to traditional laminated composites and are not applicable to 3D woven composites. This is due to complex architecture of 3D woven composites that provide through-thickness reinforcement and eliminate delamination as a

failure mechanism. To date, meso-scale representative volume element (RVE) and homogenization techniques have been developed to determine elastic properties of 3D woven composites that can be used in macro-scale models [6], [11]. However, progressive failure modeling efforts have been limited to the meso-scale which is computationally expensive [12] and provides a level of detail not required for typical structural analysis of components and assemblies.

The overall goal of this study was to develop an experimentally validated macro-scale finite element material model [6] to capture the progressive failure behavior of 3D woven composites. Specific goals for the material model developed were to: 1) ensure it can be calibrated from standard experiments, such as those defined by ASTM standards [8]-[10]; and 2) not suffer from pathological mesh dependence in modeling softening behavior [7]. For validation, 3D woven composite beams were manufactured for this study and tested to complete failure in 3-point bending. The material model developed was first calibrated using coupon level testing data and then used to simulate the experiment. The predicted load-deflection curve, peak load, and energy absorption were compared against the experimental data.

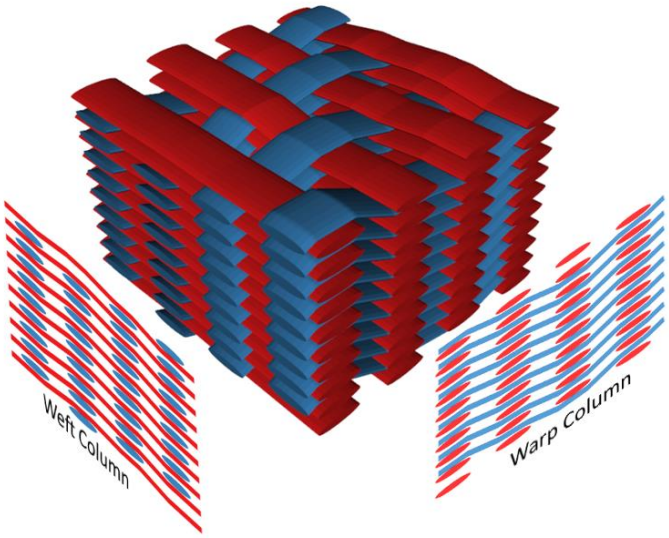

Figure 1: Representative volume element (RVE) of a 3D woven composite with ply-to-ply architecture. Warp yarns are blue and weft yarns are red. Warp and weft slices are shown on the corresponding faces of the 3D preform rendering.

2 MATERIAL MODEL DEVELOPMENT

Experimental data shows that 3D woven composite parts possess very different behaviors in tension, compression, and shear (Figure 2). When submitting a specimen to the compressive test ASTM D6441 [8], we observe little deviation from linear behavior up to failure. A similar specimen subjected to tensile test ASTM D3039 [9] exhibits a clear inflection point where the response ceases to be linear-elastic prior to failure. Finally, the v-notch rail shear test ASTM D7078 [10] shows the shear behavior to be nonlinear. In all different loading cases, unloading exhibits permanent plastic setting, and degradation of the elastic moduli when reloading. Note that properties may be quite different in the warp and weft directions depending on the weave architecture. Also, the full characterization of 3D

woven composite parts requires testing the through-thickness tensile, compressive and shear responses.

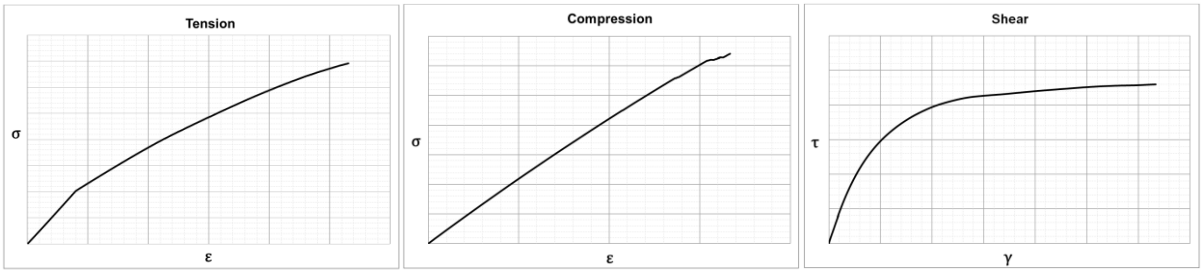

Figure 2: Experimental stress-strain curves for 3D woven composites in tension (left), compression (middle), and shear (right). Tests were quasi-static and carried out to failure and do not show unloading behavior.

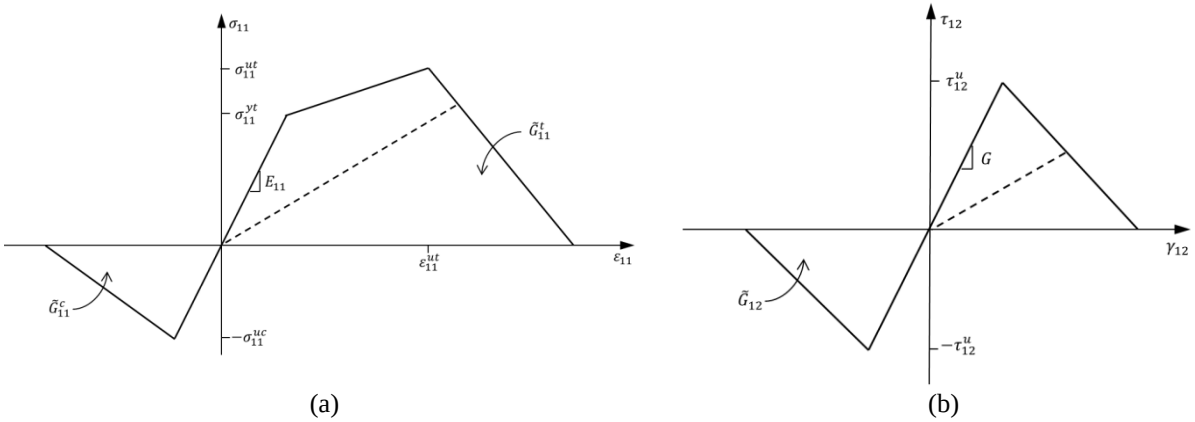

(a) (b)

Figure 3: Modeled behavior of 3D woven composite material. a) Uniaxial response in the warp or weft direction. b) Shear response on the warp-weft plane. Dotted lines shows unloading/reloading curve with no permanent set.

We modeled the elastic response of the composite as orthotropic, characterized by: the Young's modulus in the warp direction, E_{11}, the Young's modulus in the weft direction, E_{22}, the through-thickness modulus, E_{33}; Poisson's ratios ν_{12}, ν_{13}, and ν_{23}; and shear moduli G_{12}, G_{13}, and G_{23}.

Based on experimental data, the compressive behavior was modeled as linear elastic, with ultimate strength denoted by σ_{11}^{uc} for the warp direction response. At this point the material softens and dissipates the fracture energy $\tilde{G}_{11}^{c}$, as depicted in Figure 3. Weft and through-thickness compressive uniaxial responses were similarly modeled, with ultimate strengths σ_{22}^{uc} and σ_{33}^{uc}, and fracture energies $\tilde{G}_{22}^{c}$ and $\tilde{G}_{33}^{c}$, respectively.

Tensile behavior was modeled as linear elastic until yield stress is reached (σ_{11}^{yt} for the warp direction), then linear until the ultimate strength σ_{11}^{uc} at the ultimate strain ε_{11}^{uc}, followed by a softening branch. Again, weft and through-thickness responses are modeled similarly. Unloading past the linear elastic range leads to permanent stiffness degradation, depicted by the dashed line above.

Shear response was considered linear elastic until it reaches an ultimate strength, τ_{12}^{t} in the warp-weft plane, followed by softening upon further loading. Unloading once the shear stress has passed the ultimate strength leads to damaged permanent stiffness degradation.

Traditional commercial finite element analysis tools do not include built-in materials that capture all of the characteristics listed above. We therefore implemented a user defined material subroutine to be used within Abaqus/Explicit (Dassault Systemes Simulia Corp., Providence, RI), where we used the fracture energy as one of the input material parameters. Objectivity of the mechanical dissipation with different levels of mesh density was enforced by modifying the corresponding softening modulus with a characteristic length scale related to element size [4].

3 MODEL VALIDATION

3.1 Experimental Setup

In order to demonstrate the load carrying and energy absorption capabilities of 3D woven composites, a 3-point bending test of a structural beam was conducted (Figures 4 & 5). The samples used in this study were manufactured by Albany Engineered Composites (AEC). The preforms were woven using Hexcel IM7 48K carbon fiber yarns on a computer controlled 3D Jacquard weaving loom. The fiber architecture chosen was a ply-to-ply design tailored to have 60% of the fiber in the warp direction and a 60% fiber volume fraction. 60%/40% distribution of warp/weft fiber was to improve the stiffness and strength of the beam along its length, i.e. the warp direction. The weave design and program code generation was completed using AEC's proprietary software Techniweaver™. The parts were molded through resin transfer molding (RTM) using Cycom PR520 epoxy resin. The finished parts were tested to failure using a hydraulic test system under displacement control quasi-statically at a rate of 8 mm/s. The force-displacement curve and maximum load were recorded for each sample tested.

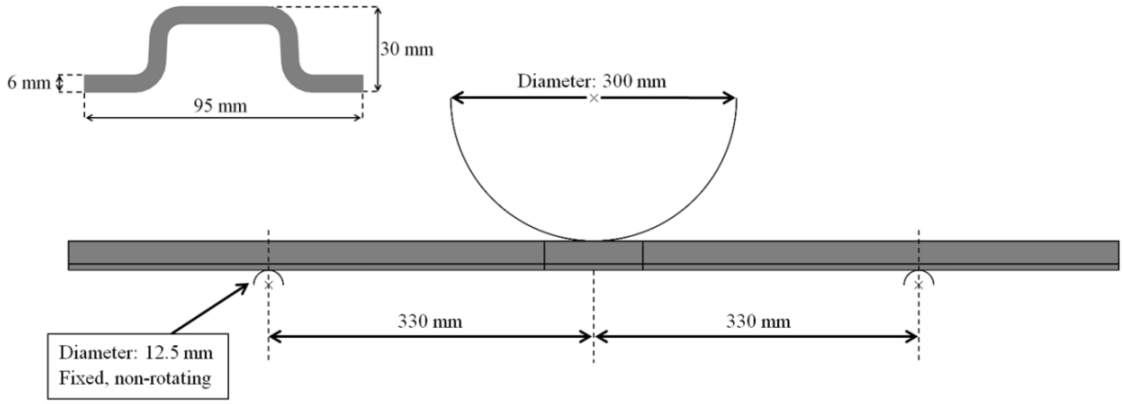

Figure 4: Experimental setup of 3-point bending test of a 3D woven composite beam. The same setup was used for the FEA model.

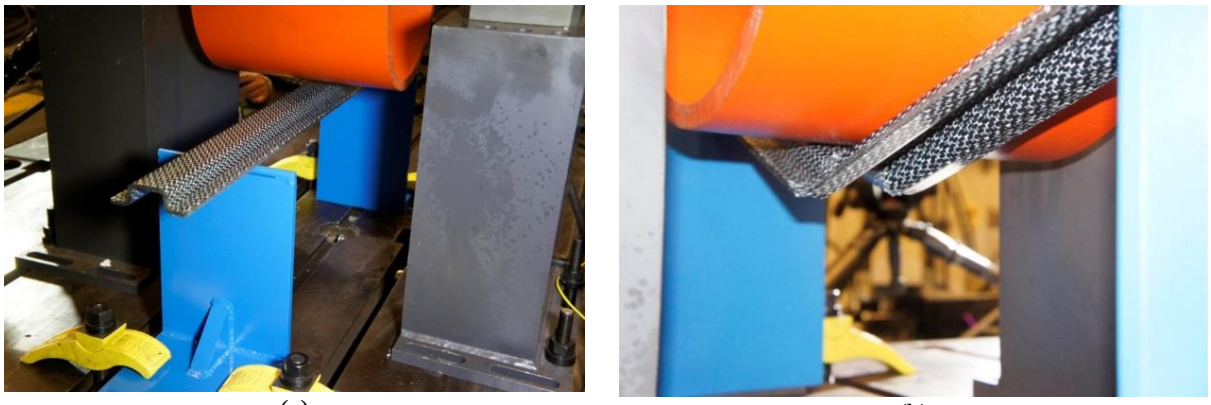

(a) (b)

Figure 5: Photographs showing the 3D composite beam 3-point bending experiments: (a) at the beginning of testing, and (b) after complete failure. The composite beam was not painted and therefore the carbon fiber and near white resin are clearly visible.

3.2 FEA Model Setup

The finite-element model consisted of 4-noded shell elements with reduced integration (S4R) to model the composite beam throughout the span, with the exception of the region underneath the impactor, where failure is predicted to take place (Figure 6). In that region, a finer mesh comprised of 8-noded continuum-shell elements was used, with 6 elements through the thickness. Shell-to-solid coupling was used to couple neighboring elements of different topologies. The impactor and supports were modeled as half-cylinders using 4-noded rigid elements. Frictionless contact was assumed between the beam, supports, and impactor. The impactor was displaced 100mm downward from its initial position touching the beam, through imposed displacement using the amplitude curve

$$u(t) = -100\left(\frac{t}{0.05}\right)^3 \left(10 - 15\left(\frac{t}{0.05}\right) + 6\left(\frac{t}{0.05}\right)^2\right) \quad (1)$$

which ramps up the displacement smoothly. The quasi-static analysis was run using the explicit dynamic procedure in Abaqus/Explicit with mass scaling to increase stable time increments and reduce total computation time. The displacement and vertical reaction force at the impactor reference node were used for post-processing.

4 RESULTS

The simulation results showed that after the initial elastic response, first failure of the 3D woven composite material occurred along the top of the beam at the region underneath the impactor where compressive stresses along the warp direction on the reach the ultimate compressive stress (Figures 5 & 6). After this, the area of compressive strain softening on the top of the beam remains restricted to a narrow band, while the stress along the warp direction reaches the inelastic tensile limit on the bottom flanges as the beam continues to deform. The area of tensile inelastic response spreads until the ultimate tensile stress is attained at the middle of the beam. At this point the beam reaches its maximum sustainable load, i.e., further

displacement of the impactor leads to lower reaction force. These observations were qualitatively consistent with the experiment.

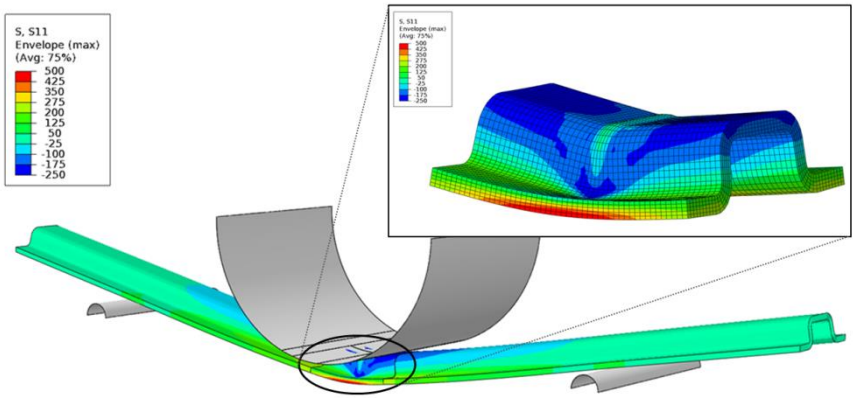

Figure 6: FEA model of the 3-point bending test setup. The inset shows mesh detail and σ_{11} distribution in continuum-shell elements (Abaqus S8R) under the impactor region.

Force-displacement curves obtained from the simulation and experiment showed very good overall correlation (Figure 7). The FEA model successfully predicted the initial elastic response, peak load, and softening behavior of the beam up to the 50mm displacement of the impactor. A slight deviation after 50 mm is observed. The overall energy absorption, i.e., the area under the force-displacement curve is in close agreement (Figure 7).

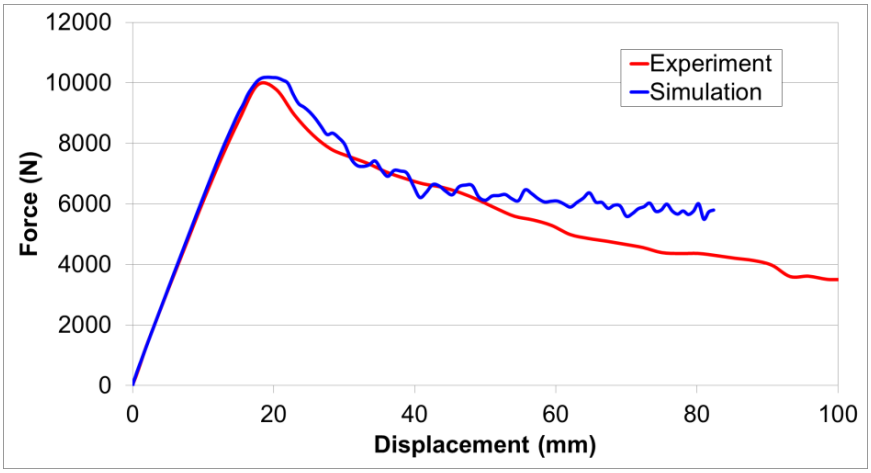

Figure 7: Comparison of one representative experimental and the FEA model force-displacement curves. The model shows very close correlation with the experiment up to the 50 mm displacement predicting the maximum load.

5 CONCLUSIONS

The main goal of this study was to develop a macro-scale FEA material model to capture the progressive failure behavior of 3D woven composites and validate it against experimental data for a 3-point bending application. Most parameters required by the material model developed were calibrated using standard experimental test data for tension, compression, and shear. Finally, the material model was implemented such that the progressive failure behavior was mesh independent by including a characteristic length scale which is present in the model.

For the quasi-static 3-point bending application in this study, permanent deformation effects were much smaller than the loss of stiffness; therefore we only considered these damage effects. This may not be a valid assumption for general applications. As such, adding plasticity to our models is part of future enhancements.

The results of the 3-point bending simulation showed very close agreement with the experiment in both the progression of failure and the overall load-displacement response (Figures 5-7). The force-displacement curve showed differences after a 50 mm displacement of the impactor, causing the model to slightly over predict the energy absorption. Overall, the results of this study indicate that despite some limitations, the material model developed can be successfully used in the design and analysis of 3D woven composites structures undergoing progressive failure.

REFERENCES

[1] Tong, L., Mouritz, A.P., and Bannister, M. *3D reinforced polymer composites*, Elsevier, 2002.

[2] Tan, P., Tong, L.Y., Steven, G.P., Ishikawa, T. Behavior of 3D orthogonal woven CFRP composites. Part I. Experimental investigation. Compos Part A – Appl Sci Manuf (2000) 31: 259-271

[3] McIlhagger, R., Quinn, J.P., McIlhagger, A.T., Wilson, S., Simpson, D., Wenger, D. The influence of binder tow density on the mechanical properties of spatially reinforced composites. Part 1 – Impact resistance. Compos Part A – Appl Sci Manuf (2007) 38: 795-801

[4] McIlhagger, R., Quinn, J.P., McIlhagger, A.T., Wilson, S., Simpson, D., Wenger, D. The influence of binder tow density on the mechanical properties of spatially reinforced composites. Part 2 – Mechanical properties. Compos Part A – Appl Sci Manuf (2008) 39: 334-341

[5] McClain, M. and Goering, J. Rapid assembly of fiber preforms using 3D woven components. *Proceedings of SAMPE 2012*, Baltimore, MD, 2012.

[6] Lomov, S.V., Ivanov, D.S., Verpoest, I., Zako, M., Kurashiki, T., Nakai, H., and Hirosawa, S. Meso-FE modelling of textile composites: Road map, data flow and algorithms. Composites Science and Technology (2007) 67: 1870-1891

[7] Simo, J.C., Oliver, J., and Armero, F. An analysis of strong discontinuities induced by strain-softening in rate-independent inelastic solids. Computational Mechanics (1993) 12:

277–296

[8] ASTM Standard D6441, Standard test method for compressive properties of polymer matrix composite materials using a combined loading compression test fixture. ASTM International, West Conshohocken, PA, 2004.

[9] ASTM Standard D3039, Standard test method for tensile properties of polymer matrix composite materials. ASTM International, West Conshohocken, PA, 2004.

[10] ASTM Standard D7078, Standard test method for shear properties of composite materials by v-notched rail shear method. ASTM International, West Conshohocken, PA, 2004.

[11] Bayraktar, H., Ehrlich, D., Scarlat, G., McClain, M., Timoshchuk, N., Redman, C. Forming and performance analysis of a 3D woven composite curved beam through meso-scale FEA, submitted to SAMPE 2014, Seattle, WA, 2014.

[12] Jia, X., Xia, Z., Gu, B. Nonlinear viscoelastic multi-scale repetitive unit cell model of 3D woven composites with damage evolution. Intl J of Solids and Struct (2013) 50: 3539-3554.